IL NUOVO CIMENTO **41 C** (2018) 188
DOI 10.1393/ncc/i2018-18188-2

Colloquia: IWM-EC 2018

Equilibration chronometry and reaction dynamics

A. Rodriguez Manso([1]), A. B. McIntosh([1]), K. Hagel([1]), L. Heilborn([1])([2]), A. Jedele([1])([2]), A. Wakhle([1]), A. Zarrella([1])([2]) and S. J. Yennello([1])([2])

([1]) *Cyclotron Institute, Texas A&M University - College Station, TX 77843, USA*
([2]) *Chemistry Department, Texas A&M University - College Station, TX 77843, USA*

received 3 December 2018

Summary. — Heavy-ion collisions exhibit a complex and beautiful variety of behavior which arises from the dynamic interplay of competing forces. The nuclear equation of state governs this behavior, and by studying this behavior we have formed an understanding of the equation of state. The low-density neck which is very pronounced in heavy-ion collisions below the balance energy plays many roles. The neck acts as a sink for neutrons, and also acts as a bridge to allow neutron-proton equilibration and mass exchange between the reaction partners. The material in the neck can be released as free nucleons, or can aggregate into clusters. The neck will rupture at least once as the reaction partners re-separate, but can rupture in multiple places with measurable delay between the ruptures. We have recently characterized neutron-proton equilibration in heavy-ion reactions in an unprecedented level of detail. We examine here the measured composition of the remnant of the projectile and the largest remnant of the neck. These compositions show both a clear dependence with rotation angle, and as the heavy fragment becomes more neutron-rich, the light fragment becomes less neutron-rich. The rotation angle is interpreted as a measure of the duration of contact; not only is a timescale extracted for neutron-proton equilibration but it is observed that the composition changes exponentially in time, consistent with a process following first-order kinetics. The results are robust with respect to the impacts of secondary decay, the background of statistical decay, and choice of alignment angle definition. The equilibration is seen for a broad range of final states and for beam and target combinations with varying initial neutron richness.

The nuclear equation of state governs the thermodynamic state variables for nuclear matter with various implications in its understanding from microscopic to astronomical phenomena. The symmetry energy is the portion of the nuclear equation of state describing the penalty for having a relative excess of neutrons or protons. The density dependence of this energy penalty is the least constrained term in the nuclear equation of state, with several probes used to study its dependence (*i.e.*, isoscaling, isospin diffusion, neutron-proton ratios and neck dynamics [1-4]). Recently, the time-dependence of neutron-proton equilibraton has re-emerged as an additional probe [5-14].

The general physics picture presented in this proceeding comprises a projectile and a target in a deeply penetrating contact. As the excited Projectile- and Target-Like Fragments (PLF* and TLF*, respectively) begin to separate, a low-density neck of nuclear material (preferentially neutrons) forms between them. The velocity gradient stretches the system and competition between velocity gradient and surface tension amplifies instabilities until the system stretches beyond the capabilities of the nuclear force to hold it together, and it ruptures. The now separated PLF* and TLF* are prone to be strongly deformed along the separation axis. In this work, we focus only on the PLF* which, due to deformation, rotation and velocity gradients, is likely to break again into what we refer to as HF (Heavy Fragment) and LF (Light Fragment). Considering the neck is neutron-rich at the time of the first breakup, nucleon flow within regions of the deformed PLF* allows neutron-proton equilibration to follow between the developing HF and LF. Hence, measuring the composition of the fragments as a function of the rotation angle grants direct observation of the time dependence of the neutron-proton equilibration [13, 14].

The experiments studied in this work [13] are the symmetric ^{70}Zn, ^{64}Zn and ^{64}Ni reactions and asymmetric ^{64}Zn+^{64}Ni at 35 MeV/nucleon using NIMROD [15] and the K500 Cyclotron at the Texas A&M University. The Neutron Ion Multi-detector for Reaction Oriented Dynamics (NIMROD) provides excellent isotopic ID for charged particles at least up to $Z = 17$ and nearly complete geometrical coverage over the angular range from 3.6° to 167°.

To examine the strong alignment expected from dynamical decays we look at the distribution of the alignment angle, α, between the center of mass velocity and the relative velocity of the HF and LF. Figure 1 (left panels) shows the normalized angular distribution for the ^{70}Zn+^{70}Zn system for three representative combinations of HF and LF. The angular distribution is peaked for the most aligned configuration and decreases in yield with decreasing alignment, where the excess yield is largest and most strongly aligned for the most asymmetric splits. Less aligned decays represent longer decay times. The total yield can be understood as a combined contribution of two different mechanisms of production: statistical decay and dynamical decay. The observed yield in fig. 1 (left panel) for $\alpha > 90°$ comes primarily from statistical decay from a rotating source, which produces an angular distribution that is symmetric about 90°. The excess yield for $\alpha < 90°$ is consistent with dynamical decay, which is very rapid, dominates at small angles and decreases in probability as α increases. Nevertheless, the larger yield observed for $\alpha < 90°$ cannot be attributed solely to either dynamical or statistical decay. To disentangle we describe the total yield as the sum of the statistical and dynamical components, we assume the statistical yield is symmetric at about 90° and that the yield above 108° is entirely statistical. Those are estimates.

For each pairing, the asymmetry was calculated as a function of the alignment angle, shown in fig. 1 (middle panels). To explore the impact of the statistical yield on the trends observed in the overall composition, we introduce a technique to extract the dynamical component of the composition as a function of α. We express the observed composition as a combination of the composition of the dynamical and the statistical components, each weighted by their fractional yield. As the angle of rotation increases, ΔHF (ΔLF) starts off very neutron-poor (neutron-rich), then evolve towards each other. The variation of the composition as a function of the alignment angle shows an exponential behavior following the parametrization $\langle\Delta\rangle = a + be^{(-c\alpha)}$ for both the HF and LF, suggesting first-order kinetics. The exponential fits of the overall composition are reproduced in the dynamical fig. 1 (right panel) for visual comparison. The dynamical composition generally follows the same trend as the overall composition, although slightly more extreme (*i.e.*, the LF

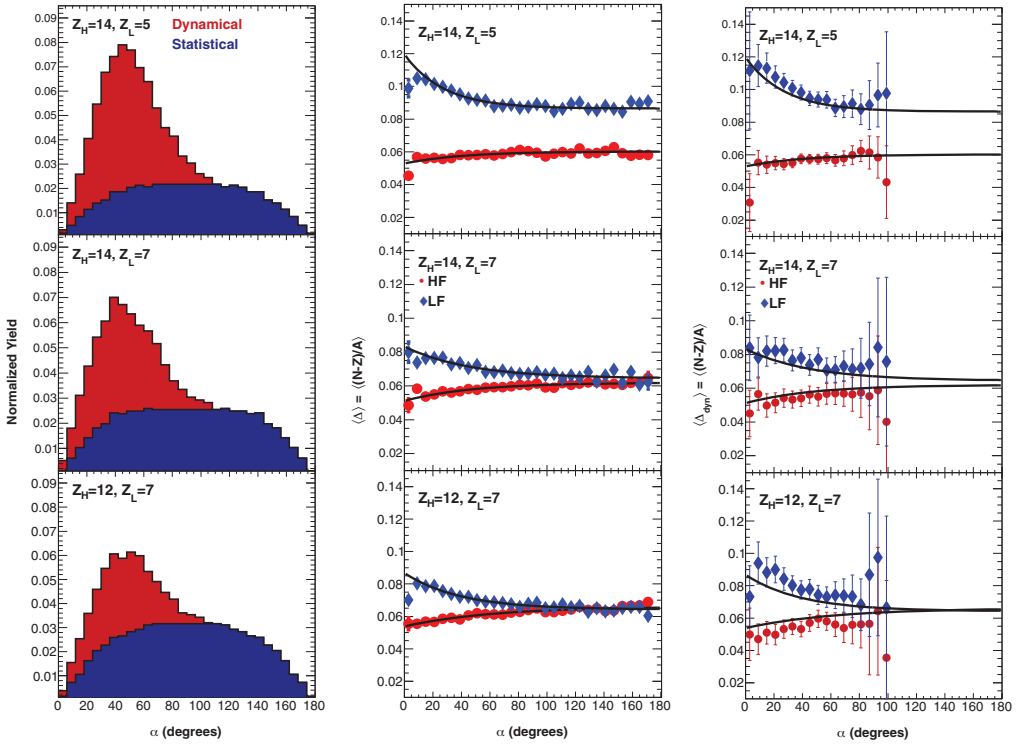

Fig. 1. – Representative combinations of HF and LF: $Z_H = 14$, $Z_L = 5$ (upper), $Z_H = 14$, $Z_L = 7$ (middle) and $Z_H = 12$, $Z_L = 7$ (lower) panels, respectively, for the ^{70}Zn+^{70}Zn system [13]. Left panels: Normalized angular distributions α where the blue area represents the statistical contribution while the red area represents the dynamical one. Middle panels: Average composition $\langle\Delta\rangle$ as a function of the decay alignment α. Right panels: Average dynamical composition, $\langle\Delta_{dyn}\rangle$, as a function of the decay alignment α. The black lines correspond to the exponential fit of the average composition as a function of the decay alignment.

is slightly more neutron-rich and the HF is slightly less neutron-rich). Considering that applying this correction to separate the dynamical component results in significantly larger uncertainties and that the rate of change of the composition is approximately unaffected by the correction, we continue the analysis on the inclusive composition rather than the dynamical one.

Subsequent to the PLF* breakup, HF and LF can be in excited states and possibly undergo light particle secondary decay (*i.e.*, n, p and α), hence the interest in studying secondary decays and how it affects the average composition as a function of the alignment angle, for which we used GEMINI++ simulations [16]. The results are shown in fig. 2. We studied correlations prior to secondary decays and correlations of the final-state fragments. Variation of the initial excitation energy maintained the exponential dependence of the average composition as a function of the alignment angle, although a change to lower composition and a muting of the amplitude that is stronger for higher excitation energy is observed. Varying the starting average composition showed that the system with initially larger asymmetry was shifted down strongly by secondary decays (consistent with the picture of a system farther from the valley of stability feeling a stronger force driving it back toward the valley). After secondary decays, the more neutron-rich system continued to be more neutron-rich. In conclusion, secondary decays can modify

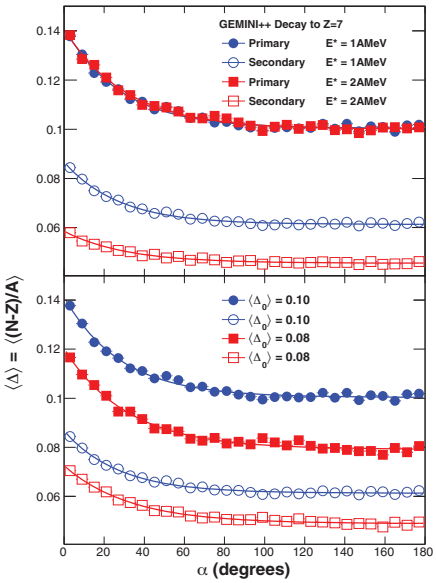

Fig. 2. – GEMINI++ simulations show the effects of secondary decay on the composition $\langle\Delta\rangle$ as a function of the alignment angle α [13]. Full markers show initial composition and open markers show the composition after secondary decay. The upper panel shows the effect of varying the excitation energy. The lower panel shows the effect of varying the initial composition from neutron-rich to less neutron-rich system.

the composition we observe, but crossings of the ΔHF with ΔLF or gaps between them do not necessarily contain any more physical meaning than that coming from secondary decay. The trend in the average composition as a function of the alignment angle is not destroyed or created, and the distinctive rate of the exponential is maintained.

Up to now, we focused on results from collisions of the symmetric ^{70}Zn system, therefore, we expand our study to other projectiles and targets. Figure 3 shows the average composition as a function of the decay alignment for the $Z_H = 12$, $Z_L = 7$ pair, not only for the ^{70}Zn+^{70}Zn system, but also for the ^{64}Ni+^{64}Ni, ^{64}Zn+^{64}Zn and ^{64}Zn+^{64}Ni

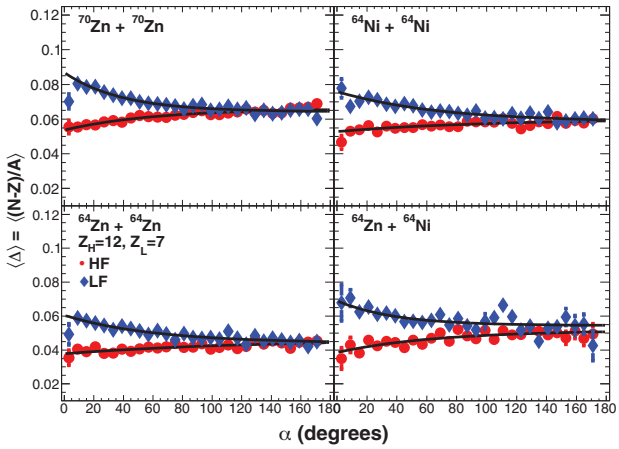

Fig. 3. – Average composition $\langle\Delta\rangle$ as a function of the decay alignment α for the $Z_H = 12$, $Z_L = 7$ pair in all systems studied [13].

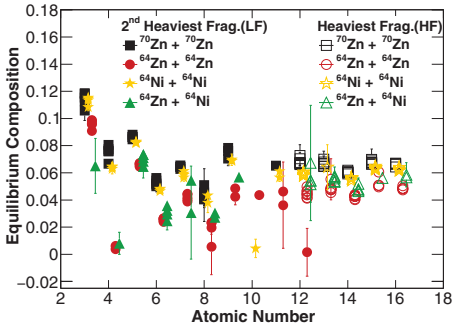

Fig. 4. – Equilibrium composition as a function of the atomic number for all four systems studied [13].

systems. The black lines correspond to the exponential fits of the data. From the figures, it is observed that the Δ/α (^{70}Zn, ^{64}Ni) correlations are essentially the same. The ^{64}Zn system is less neutron-rich than the other two symmetric systems, accordingly, the Δ/α (^{64}Zn) correlation is shifted to lower equilibrium composition values, although the rate constants and change from initial to final values remain the same. Comparing the symmetric and the asymmetric systems, the Δ/α correlation for the symmetric system is systematically lower, supporting the observance of target effects.

Focusing on the exponential fits of the data, the parameter a is the equilibrium of the composition with respect to the rotation angle. Figure 4 shows the equilibrium composition as a function of the atomic number for all the systems studied. The error bars reflect the uncertainty due to the fitting procedure. The position of the points in the x-axis of the graph is offset slightly for each system to facilitate visualization of the results. The Z_L and the Z_H values are fairly clustered, which implies that the equilibrium value for the LF (HF) depends on the Z_L (Z_H) but not on the Z_H (Z_L). This is consistent with dependence on available isotopes for a specific Z_H and Z_L. Comparing the symmetric ^{70}Zn (in black squares) and the ^{64}Ni systems (in yellow stars), which have similar neutron-rich system composition, both show approximately the same equilibrium composition

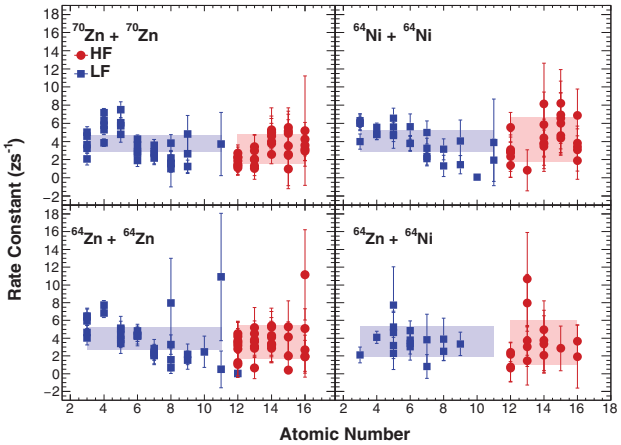

Fig. 5. – Rate constants (in units of inverse zs) as a function of the atomic number for all four systems [13]. The red circles represent the atomic numbers of the HF while the blue squares represent the atomic numbers of the LF. The shaded areas correspond to the average rate constant per zs values for the HF and LF.

for all daughters. The ^{64}Zn (in red circles), which has fewer neutrons overall, shows consistently less neutron-rich equilibrium compositions for all daughters. On average, the asymmetric system ^{64}Zn+^{64}Ni (in green triangles) has slightly more neutron-rich daughters than the neutron-poor system (in red) and slightly less neutron-rich daughters than the neutron-rich systems (in black and yellow). Albeit error bars being significant in several cases, such systematic behavior is consistent with the expected neutron-rich target effects.

In the fits, the parameter c (*i.e.*, the exponential slope) is a surrogate of the rate constant for equilibration with respect to the rotation angle. Figure 5 shows the rate constants (in units of inverse zs) as a function of the atomic number for the symmetric and the asymmetric systems studied. The rate constant is the relevant parameter to calculate the equilibration times and describes how quickly the equilibration occurs within the PLF*. We use the angular velocity to convert the rotational angle into time. The agreement in the rate constants, not only comparing the HF and LF but also among different systems, indicates that the mechanism driving the equilibration is independent of the size of both partners and the systems studied (charge, mass, or composition), and as a consequence, depends only on the difference in chemical potential (*i.e.*, asymmetry).

In summary, we studied the time dependence of the neutron-proton equilibration by examining the composition of the fragments emitted from the PLF* as a function of the alignment angle, which serves as a clock for the equilibration. The composition follows an exponential behavior suggesting first-order kinetics for all the systems studied. We extracted a purely dynamical composition component. The difference in the observed composition for reactions of a relatively neutron-poor projectile with a neutron-rich target shows a small systematic effect. This effect does not have an influence in the rate constants hence, in the mechanism driving the equilibration.

* * *

This work is supported by the Robert A. Welch Foundation (Grant A-1266) and the U.S. Department of Energy DOE (Grant DE-FG02-93ER40773). We are thankful to the staff at the Texas A&M University Cyclotron Institute for providing the excellent quality beams and technical support that made this work possible.

REFERENCES

[1] Bao-An and Ko C. M., *Phys. Rev. C*, **57** (1998) 2065.
[2] Theriault D. *et al.*, *Phys. Rev. C*, **74** (2006) 051602.
[3] Galichet E. *et al.*, *Phys. Rev. C*, **79** (2009) 064614.
[4] Galichet E. *et al.*, *Phys. Rev. C*, **79** (2009) 064615.
[5] Moretto L. and Schmitt R., *Rep. Prog. Phys.*, **44** (1981) 533.
[6] Planeta R. *et al.*, *Phys. Rev. C*, **38** (1988) 195.
[7] De Filippo E. *et al.*, *Phys. Rev. C*, **71** (2005) 044602.
[8] De Filippo E. *et al.*, *Phys. Rev. C*, **86** (2012) 014610.
[9] Hudan S. *et al.*, *Phys. Rev. C*, **86** (2012) 021603.
[10] Brown K. *et al.*, *Phys. Rev. C*, **87** (2013) 061601.
[11] Stiefel K. *et al.*, *Phys. Rev. C*, **90** (2014) 061605.
[12] Hudan S. *et al.*, *Eur. Phys. J. A*, **50** (2014) 36.
[13] Rodriguez Manso A. *et al.*, *Phys. Rev. C*, **95** (2017) 044604.
[14] Jedele A. *et al.*, *Phys. Rev. Lett.*, **118** (2017) 062501.
[15] Wuenschel S. *et al.*, *Nucl. Instrum. Methods A*, **604** (2009) 578.
[16] Charity R., *Phys. Rev. C*, **58** (1998) 1073.